ACS OMEGA

http://pubs.acs.org/journal/acsodf

Article

Combustion Performance of Agropellets in an Experimental Fixed Bed Reactor versus a Commercial Grate Boiler. Validation of Ash Behavior

Sebastián Zapata,* Paula Canalís, Javier Royo, Maider Gómez, and Carmen Bartolomé

Cite This: *ACS Omega* 2023, 8, 29485−29499

Read Online

ACCESS | Metrics & More | Article Recommendations | Supporting Information

ABSTRACT: Agrobiomass is presented as a suitable alternative to contribute to the fossil fuel decarbonization strategy at the European level. To achieve the ambitious objectives established in this regard: (i) new biomass resources need to be used and therefore initially tested in order to confirm its potential for different applications, such as energy production, and (ii) biomass supply capacity needs to be enlarged; therefore, agroindustries converted into Integrated Biomass Logistic Center (IBLC) can play a key role. In this research, eight different agropellets (blends of wheat straw and maize stalk with forestry wood) were produced in a IBLC and tested in a commercial boiler, comparing the results with previous ones obtained in a fixed bed reactor test campaign and to a base case (woody pellets). This paper includes both individual results in terms of bottom ash, deposition, and a final comparison of ash behavior in both facilities. All biofuels tested showed an adequate performance in terms of efficiency and emissions, being slightly better for the agropellets produced with wheat straw. Regarding sintering and deposition, the tendencies found in the reactor investigation were also observed in the commercial boiler. Moreover, the assessment of the results from the boiler and reactor's tests proved that reactor experiments are representative and may be used to test new biofuels more efficiently in terms of effort and time allocated and could be used to predict sintering and deposition phenomenon occurrence.

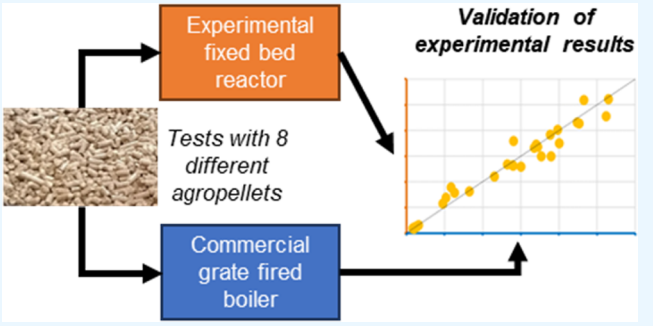

1. INTRODUCTION

Decarbonization and climate change mitigation are presented as challenging goals for industrial sectors in Europe. Recently, the European Commission launched the legislative initiative "Fit for 55" in July 2021.[1] The package contains legislative proposals to revise the entire EU 2030 climate and energy framework, addressing the legislation on effort sharing, land use and forestry, renewable energy, energy efficiency, emission standards for new cars and vans, and the Energy Taxation Directive. Previously, Red II defined the overall EU target for renewable energy source consumption by 2030.[2] In order to reach these decarbonization objectives established for 2030 and 2050, it is crucial to find and test new sources of residual biomass fuels, which could be able to compete and/or substitute fossil fuels and traditional biomass sources, such as forest biomass.

The main challenge concerning these new biofuels relates to ash content and their composition, which can lead to deposition and sintering. It is therefore necessary to deeply study their behavior during combustion and how to address these phenomenon occurrence to decrease their impact on the overall performance and efficiency.

Ash undergoes physical and chemical transformations during combustion. Part of the ash components accumulates on the grate (bottom ash) and, given the low ash melting temperature of many residual biomass fuels, can sinter and cause significant problems in terms of emissions as well as efficiency and equipment lifetime decrease.[3−7] The ash that is not retained in the bed (fly ash) can leave it by means of two different mechanisms: vaporization or entrainment of solid particles (coarse fly ash). After complex mechanisms,[8−10] a fraction of this volatilized ash can directly condense or, after forming aerosols, be deposited by thermophoresis and/or diffusion[9,11,12] on the heat exchange surfaces of the equipment. It can even condense into coarse fly ash.[9,11] On the other hand, part of the coarse fly ash can be deposited on heat exchange surfaces by inertial impact. All these deposits can cause a reduction of the heat transfer, and an increase of corrosion and erosion phenomena.[3−7]

Within this context, pilot facilities can play a key role enabling to learn more about the performance of these new biofuels, which in turn could contribute to expand their use. This kind of

Received: May 9, 2023
Accepted: July 25, 2023
Published: August 4, 2023

https://doi.org/10.1021/acsomega.3c03201
ACS Omega 2023, 8, 29485−29499

Table 1. Bibliography Studies in Lab-Scale Reactors

Objective	Technology	References
Examine kinetics of loose biomass combustion seeking to study heat- and mass-transfer processes and the impact of flue gas recirculation on the peak temperature	Vertical tube reactor	13
Analyse fouling on heat exchangers	Lab-scale combustor with underfeed fixed-bed and air staging	14
Study of the ignition front propagation velocity and the impact of the excess air ratio	Fixed-bed combustor	15
Evaluate combustion characteristics and process rates	Fixed bed reactor	16
Study the dynamic behavior of ash deposition	Down-fired furnace	17
Evaluate the deposition behavior and fouling phenomena	Entrained flow reactor	18
Comparison of silica and limestone as bed materials to reduce agglomeration and sintering tendencies	Bubbling fluidized bed	19
Quantify the release of K, Cl, S, and P during combustion	Fixed-bed reactor	20
Evaluate combustion performance and study ash behavior (sintering and deposition)	Fixed-bed reactor	21

Table 2. Fuel Properties (% a.r.: Weight Percentage as Received; % d.b.: Weight Percentage in Dry Basis)

Parameter	Units	WP100 Wood pellet 100%	WSP100 Wheat straw pellet 100%	WSP72 Wheat straw pellet 72%	WSP60 Wheat straw pellet 60%	WSP35 Wheat straw pellet 35%	MSP100 Maize stalk pellet 100%	MSP52 Maize stalk pellet 52%	MSP10 Maize stalk pellet 10%
					Proximate Analysis				
Moisture	% a.r.	7.6	4.8	6.4	6.7	10.2	5.5	5.5	7.6
Volatile matter	% d.b.	81.0	73.8	74.5	74.9	74.7	71.7	72.9	74.8
Fixed carbon	% d.b.	18.0	20.1	21.6	22.0	21.2	15.8	20.9	22.1
Ash	% d.b.	1.0	6.1	3.9	3.1	4.1	12.5	6.2	3.2
Durability	% a.r.	91.3	97.7	96.6	95.9	92.6	96.1	97.4	
Bulk density	kg/m^3,d.b.	510.2	667.3	604.3	562.2	460.0	638.1	655.6	587.6
Fine percentage	<3.15 mm	3.07	1.76	3.10	1.52	4.41	2.44	0.98	1.27
					Ultimate Analysis				
C	% d.b.	51.90	45.50	48.10	49.20	49.30	42.60	48.10	51.4
H	% d.b.	5.80	5.80	5.90	6.00	5.90	5.20	5.80	5.8
N	% d.b.	0.13	0.42	0.30	0.50	0.29	0.82	0.44	0.27
S	% d.b.	0.01	0.08	0.08	0.03	0.05	0.13	0.03	0.03
Cl	% d.b.	0.02	0.19	0.06	0.05	0.05	0.53	0.20	0.06
O	% d.b.	41.00	41.91	41.66	41.12	40.32	38.20	39.23	37.7
					Heating Value				
Low heating value	kW h/kg, a.r.	4.90	4.43	4.59	4.67	4.50	4.00	4.61	4.70

facilities allow one to perform flexible and complete experimental studies, which enable to analyze the dynamic behavior of ash deposition in pure or blended biomass combustion to optimize its performance. The aim of this kind of research is to understand fuels' behavior and define the most appropriate operating parameters for each blend.

Even though it represents the most accurate method to test new fuels, combustion tests carried out in facilities with boilers are challenging and time consuming, due to the large number of variables affecting the performance and the difficulty to appropriately monitor them. For this reason, these tests are frequently carried out in lab-scale reactors, which allow one to adequately control the combustion conditions while simplifying the operation, enabling the performance of more systematic analyses, longer experimental series, and a tighter control of the conditions. The applicability of experimental reactors is supported by numerous experiences. Table 1 summarizes the characteristics and objectives of some of these experiences.

This type of reactor enables to monitor more easily the behavior of fuels under different operating conditions. Additionally, they allow samples to be taken more readily for the characterization of solid residues, which is key to assessing sintering and deposition phenomenon occurrence. Several studies have investigated the deposition phenomena in these lab-scale reactors (e.g., refs 14, 17, 18 , and 22−24) and the problems associated with biomass sintering (e.g., refs 19 and 24−27).

The rationale for the use of these reactors is to carry out tests and, based on the obtained results, extract conclusions that enable for instance to predict the behavior of different biofuels during combustion in commercial installations in terms of sintering and deposition. Nevertheless, the validation of the results obtained in these reactors by means of tests performed in boilers is rarely performed. Experiences have been carried out in boilers applying similar methodologies to the one described in the current work aiming to assess the behavior of different fuels regarding sintering[28,29] and deposition phenomena;[30,31] nevertheless, the results have not been compared with the ones achieved in reactors.

In this sense, the work carried out aims to compare and validate the results obtained in a fixed bed reactor at the lab scale with the ones achieved during the combustion tests performed in a commercial boiler, using the same fuels, aiming to verify the former's suitability to predict the importance of sintering and deposition phenomenon occurrence. The work presented in this paper has its origin in several experimental series performed in the reactor facility (see publications (refs 32 and 33), which have been compared with an experimental campaign in a boiler

https://doi.org/10.1021/acsomega.3c03201
ACS Omega 2023, 8, 29485−29499

Table 3. Ash Analysis (EN-ISO 16967:2015)

Parameter	Units	WP100 Wood pellet 100%	WSP100 Wheat straw pellet 100%	WSP72 Wheat straw pellet 72%	WSP60 Wheat straw pellet 60%	WSP35 Wheat straw pellet 35%	MSP100 Maize stalk pellet 100%	MSP52 Maize stalk pellet 52%	MSP10 Maize stalk pellet 10%
Na_2O	% d.b.	1.5	0.27	0.58	0.51	0.89	0.64	0.67	1.17
MgO	% d.b.	9.06	3.04	2.86	2.91	2.69	7.99	6.1	6.77
Al_2O_3	% d.b.	5.62	1.19	1.75	2.13	5.88	5.81	5.82	7.00
SiO_2	% d.b.	16.55	55.81	38.11	34.57	35.00	38.94	38.38	27.71
P_2O_5	% d.b.	3.89	2.62	4.36	3.84	2.96	3.61	4.17	3.65
K_2O	% d.b.	13.27	21.71	27.52	28.48	23.87	11.05	11.75	11.29
CaO	% d.b.	41.02	9.88	17.50	20.27	21.6	21.95	24.97	35.06
TiO_2	% d.b.	0.35	0.08	0.10	0.12	0.21	0.3	0.29	0.38
Fe_2O_3	% d.b.	3.85	0.57	0.85	1.03	1.81	2.35	2.56	3.17

seeking to validate this comparison. This paper includes both individual results in terms of bottom ash, deposition, and a final comparison of ash behavior in both facilities.

2. MATERIALS AND METHODS

2.1. Fuels. Eight different biofuels were produced in an agroindustry inside the feed and fodder sector according to the AGROinLOG project[34] concept based on the promotion of Integrated Biomass Logistic Centers (IBLC) in agroindustries.

The starting point to define the blends to be used was to evaluate the available residual agricultural biomass from the surrounding area where the IBLC is located. Based on this potential availability assessment, wheat straw and maize stalk were selected to develop blended pellets together with forestry wood seeking to fulfil quality requirements (according to ISO 17225-6 Class A and B). More information on the methodology followed to design and produce agropellet blends can be found in ref 35.

As a result, eight fuels were produced and analyzed taking into account the following aspects: durability, amount of fines, bulk density, proximate and ultimate analyses, lower heating value (Table 2), and ash chemical analysis (Table 3).

2.2. Experimental Fixed Bed Reactor. The reactor used consists of a vertical cylindrical combustion chamber, a grate, an air supply system, and a weighing scale, which allowed one to monitor the reactor weight (see Figure 1). The chamber is made of steel AISI-310S. Its dimensions are 1700 mm height, 200 mm inner diameter, and 8 mm thick. The insulation placed around the side wall is made of two different materials: ceramic fiber (50 mm) and rockwool (70 mm) seeking to ensure that bi-dimensional effects are avoided almost completely besides increasing safety when operating. The primary air is supplied from below through the grate (grate porosity is 4.5%), so it is evenly distributed in the width of the reactor. The reactor has a system for air conditioning (see Figure 1), so that air is supplied at a constant temperature (25 °C), independently of the ambient conditions. The maximum bed height is 500 mm (i.e., level 1 in Figure 1). A smaller batch can be introduced (reaching only levels 2 or 3, as shown in Figure 1) when tests are carried out with a biofuel with high bulk density.

Regarding the operation, the equipment operates in the counter current mode: ignition starts at the top of the fuel bed (level 1, 2, or 3) by means of an electrical ignitor and the ignition front propagates downward, while combustion air moves upward. In order to monitor the performance, 15 N-type thermocouples can be placed along the height of the reactor enabling to measure gas temperatures up to 1250 °C. Ten of them are inserted inside the fuel bed (separated by 5 cm).

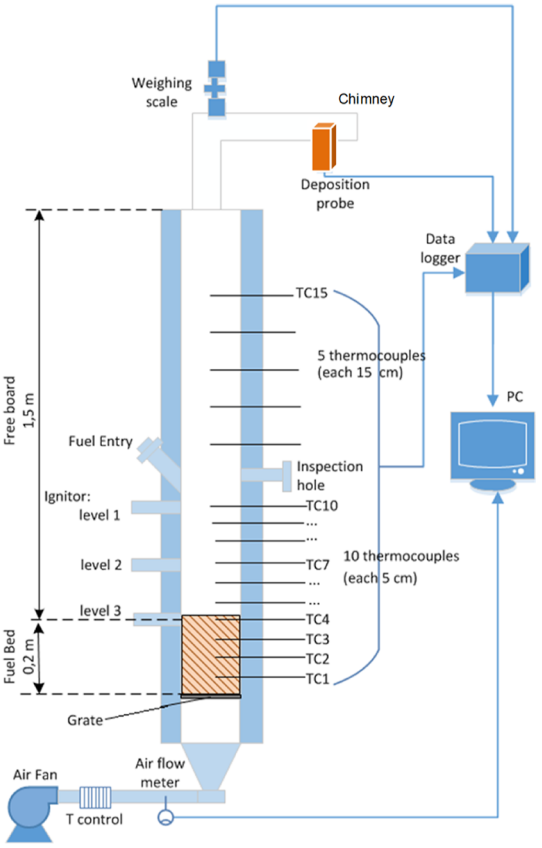

Figure 1. Scheme of the experimental test facility.

Additionally, the facility was completed by installing a deposition probe in the outlet pipe of the reactor (see Figure 1, more information is provided in this regard in Section 2.4).

2.3. Commercial Grate Fired Boiler. A 430 kWth nominal power biomass grate-fired unit, primarily adapted for the conversion of ash-rich fuels, was used to evaluate the applicability of blended biofuels for heating purposes in existing biomass units. As presented in Figure 2, the conversion system used in the experimental part of this work is mainly divided into four zones: burner (I), combustion chamber (II), and a heat exchanger section (III).

The burner is placed inside the combustion chamber and consists of two stationary main grates (see Figure 2, 5) with several holes for air supply. The first grate, which is located in the upper part of the burner, is composed of horizontally positioning small steps, resembling a ladder (with the openings in the riser

https://doi.org/10.1021/acsomega.3c03201
ACS Omega 2023, 8, 29485−29499

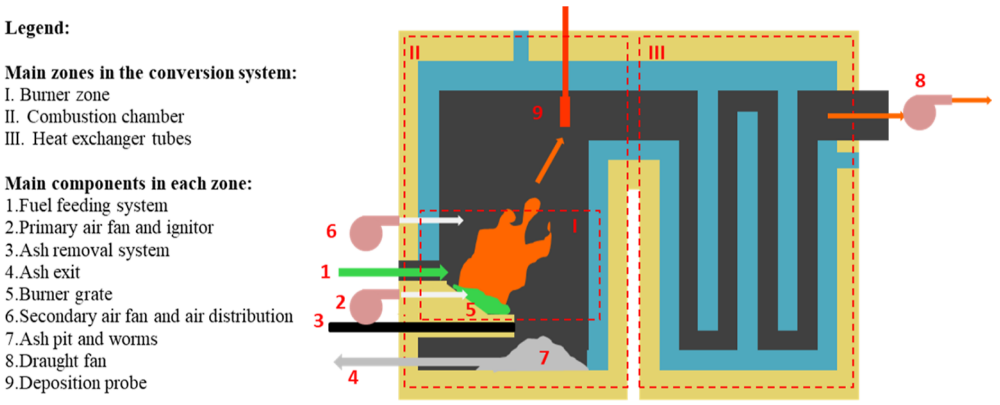

Figure 2. Main components of the grate fired conversion system.

part). The second one, which is positioned at the end of the last step, is also flat but longer to facilitate complete char burnout.

Combustion air is supplied by three different fans. Primary air (see Figure 2, 2) is provided as underfeed air through each burner grate by two independent fans, one impels primary air through the horizontal grate and other through the ladder. The air injection nozzle arrangement and their number differ in each grate step in order to supply as much air as possible according to requirements for each thermal transformation process that fuel particles undergo during combustion over the grate (i.e., heating up, drying, devolatilization, and char oxidation phases).

This burner is also designed with an automatic ash removal system (see Figure 2, 3), which scrapes ashes and other combustion residues away from the second grate and moves them into the ash pit located inside the combustion chamber (see Figure 2, 7). The working period of the ash pusher (on/off) can be adjusted according to the fuel properties' requirements, in order to both guarantee the required time for char combustion and avoid ash accumulation and severe slag and sintering occurrence over the grate. The latter function attributed to the pusher speed controller system, which contributes to provide a higher air−fuel contact over the grate, and hence enhances maximum fuel−air mixing, adapted to the fuel ash properties. In this manner, bed movement conditions on the grate are also controlled by adjustments to both the air distribution and the automatically controlled periodical ash removal under a continuous operation mode.

In order to facilitate complete mixing, as far as possible, between the air and volatilized matter released from the fuel bed on the grate, secondary air is distributed into a combustion chamber through several nozzles located in a surrounding channel above the grate (see Figure 2, 6), where secondary air is partially preheated by heat transferred to the boiler walls. This configuration allows a radial secondary air injection (see Figure 2, 6). Besides the boiler walls in the combustion chamber, the integrated heat exchanger (see Figure 2, III) is also water jacketed.

Finally, in order to control the amount of air supply and flue gas residence time during their path in the system, the force draught is automatically regulated by a fan equipped with a frequency meter (see Figure 2, 8). More detailed information on the description and the operation of the installation can be found in ref 28.

The same as in the fixed bed reactor, deposition was measured through the deposition probe (described in Section 2.4) that was introduced inside of the combustion chamber (Figure 2, 8).

2.4. Ash Analysis. For all tests performed, both reactor and boiler tests, bottom ash and fly ash were collected in order to better assess the ash behavior of each fuel under different operating conditions.

2.4.1. Evaluation of Deposition Behavior. Both facilities were completed by installing a deposition probe in the gas outlet. This is a usual device used to estimate the ash deposition in heat exchanger surfaces. It consists of a removable ring, which is cooled by compressed air, allowing to keep its surface at an appropriate temperature for deposition phenomena to occur (350 °C). Three N-type thermocouples are placed in the deposition probe to continuously measure flue gases, refrigeration air, and sampling ring temperatures during the tests. Prior to the experiment, the sampling ring is cleaned, dried, measured, and weighed. Once extracted, the dirty sampling ring is dried and weighed again to obtain the amount deposited. Using this weight value, the surface of the sampling ring, and the duration of the test, it is possible to calculate the deposition rate (DR, $g \cdot m^{-2} \cdot h^{-1}$), allowing one to estimate the deposition tendency of each studied fuel.[14,18]

In the tests carried out in the reactor, the deposition probe was placed in the chimney (see Figure 1) during the interval of stable combustion (defined in Section 3.1). In the boiler test, once the steady-state regime was reached, the probe was placed in the combustion chamber at the high-temperature zone (see Figure 2), in which the probe was positioned vertically to keep it perpendicular to the flue gas path.

In this work, the methodology exposed in ref[36] to estimate deposition by condensation ($DR_{Cond.}$) and by inertial impact (DR_{Imp}) has been applied to both reactor and boiler results. $DR_{Cond.}$ is associated with the ash that leaves the bed by vaporization and which includes the deposition by thermophoresis and diffusion; meanwhile, DR_{Imp} is associated with the ash that leaves the bed by entrainment. This methodology uses the elemental composition of the S1 fraction and of the deposits [from scanning electron microscopy−energy-dispersive spectroscopy (SEM−EDS) analysis, Section 2.4.3].

2.4.2. Evaluation of Sintering Behavior. Once combustion is completed and the reactor or boiler has cooled down, bottom ash is collected from the grate. It is weighted and classified in three fractions based on a revised classification of sintering status defined in a previous work.[37,38] The fractions are as follows:

S1: passes through a 3.15 mm sieve, and it is considered as not sintered.

S2: does not pass through a 3.15 mm sieve, but it is easily disaggregated.

https://doi.org/10.1021/acsomega.3c03201
ACS Omega 2023, 8, 29485−29499

Table 4. Summary of Reactor Test Features

		WP100	WSP100	WSP72	WSP60	WSP35	MSP100	MSP52	MSP10
Number of successful tests		10	8	8	9	10	5	8	10
λ	min	0.66	0.85	0.75	0.74	0.62	0.81	0.64	0.64
	max	1.91	1.67	1.35	1.41	1.48	1.18	1.27	1.51
	mean	1.20	1.12	1.04	1.08	1.06	0.98	0.93	1.04
T_{if} (°C)	min	935	1135	1103	1009	1100	1234	1203	1152
	max	1180	1252	1169	1136	1239	1268	1282	1268
	mean	1069	1176	1133	1091	1181	1248	1235	1230

S3: does not pass through a 3.15 mm sieve, and it is difficult to disaggregate.

Because the difference between S2 and S3 is subjective, a fraction S2/3 encompassing both classes was used. The sintering degree of a fuel will be calculated as the percentage of this last fraction with respect to the total ash was fed with the fuel in each test. The higher this percentage, the more problematic the fuel is considered.

2.4.3. Ash Chemical Characterization. After obtaining DR, a sample was taken from the front face of every removable sampling ring, that is, from the one faced perpendicular to the flow of combustion gases. Each sample was glued onto metal plates with carbon tape and then coated with carbon.

In the same way, once the sintering degree had been calculated, a sample of S1 and S2/3 bottom ash fractions were collected and crushed in a mortar to obtain a homogeneous sample with an adequate particle size. Once this process was finished, they were treated in the same way as the ones collected in the removable rings.

All the samples were analyzed by the SEM−EDS method. The equipment used is a Carl Zeiss Merlin electronic field-emission microscope equipped with a Gemini Column, with acceleration voltages between 0.02 and 30 kV, with an EDS X-MAS detector of Oxford Instruments with a window of 20 mm^2 and with resolution in energy from 127 eV to 5.9 keV. For each sample, three zones of 1 mm^2 were selected, taking the image with the retro-dispersed detector (asb). The average elemental composition was obtained through EDS with a voltage of 15 kV, being processed with the INCA software. Elements analyzed included the main participants in the most important ash transformations processes, namely, Na, Mg, Al, Si, P, S, Cl, K, and Ca.

In addition, the crystalline matter composition of S2/3 fraction and removable ring samples of some test for each fuel were determined by the P-XRD method. Standard X-ray diffraction patterns were collected at room temperature using a Rigaku D/max instrument with a copper rotating anode and a graphite monochromator to select Cu Kα wavelength. The measurements were performed at 40 kV and 80 mA, in the angular range from 5 to 80° on 2θ, applying a step size of 0.03° and a counting rate of 1 s/step. The X-ray pattern was analyzed using the JADE 7 program, with access to "JCPDS-International Center for Diffraction Database (2000)". Crystalline phases were quantified using the reference intensity ratio (RIR) method. In addition, to quantify the amorphous phase peak, decomposition was carried out through profile fitting, using a pseudo-Voigt approximation, with Lorentz = 0.5. The crystallite size of each peak (XS) was measured and the proportion of the amorphous phase was calculated, considering peaks with an XS below 80 Å to be included.

2.5. Statistical Analysis. To determine the goodness of the correlations between different parameters related to sintering and deposition obtained in the tests carried out in the reactor and in the boiler (Section 5), a statistical analysis through the estimation of the Pearson's correlation coefficient (r) and its corresponding p-value (p) was performed. The correlation will be considered statistically significant when $p < 0.05$.

3. EXPERIMENTAL TEST IN A FIXED BED REACTOR

3.1. Experimental Design and Test Features. A total of 68 tests were successfully carried out with the eight fuels (between 5 and 10 test per fuel). The inlet air temperature (T_a) was the same in all the tests (25 °C). The air inlet, expressed as the air mass flow by the unit area of the grate (PA, $kg{\cdot}m^{-2}{\cdot}s^{-1}$), was changing (range from 0.25 to 0.55 $kg{\cdot}m^{-2}{\cdot}s^{-1}$). Depending on the air flow supply, an excess air ratio (λ) lower (simulating a boiler with secondary air inlets) or higher than 1 was obtained. Both regimens are interesting to analyze the sintering phenomenon because it takes place at the bottom of the boiler. Nevertheless, when the deposition phenomenon is analyzed, which take place at the top of the boiler; the test with $\lambda < 1$ has not been considered because the combustion is incomplete (because the experimental reactor does not have a secondary air flow that guarantees the excess of air necessary in operating conditions of regular facilities).

In addition, the mean flame temperature (T_{if}, °C) was calculated. To compute this temperature, a time interval of stable combustion is defined between the instant the first TC placed inside the bed (see Figure 1) reaches 500 °C and moment TC1 (near the grate) reaches the same temperature. The mean value of the maximum temperature of these TC is T_{if}.

Based on the tests carried out in the reactor, the combustion behavior of the eight fuels could be compared and the influence of the operating conditions could be analyzed. Table 4 summarizes the main features of the tests performed. All the fuels presented adequate combustion parameters for a wide range of excess air ratio (especially the blended pellets).[32] T_{if} was higher in the tests carried out with the agropellets, reaching in these cases the maximum value around the stoichiometric air ($\lambda \sim 1$).[32] On the other hand, the MSP family presented higher temperatures and more stable than the WSP family. In the case of WP100, this temperature decreased with λ.[32]

In the following sections, only the results related to the behavior of the ashes will be shown, in order to compare them with those obtained for the same fuels in the commercial boiler.

3.2. Bottom Ash. From the tests carried out in the reactor, it was possible to analyze the influence of λ on the amount of bottom ash and its sintering degree.[32] The behavior was different for agropellets compared to the WP100 in which case both values decreased with λ. As previously mentioned, for this fuel, the T_{if} decreases with λ, which implies the decrease of the sintering degree. This fact, together with the increase of λ, leads to a greater entrainment of solid particles that causes the bottom ash to decrease. For the rest of the fuels, the bottom ash was not affected by λ, while in the case of the sintering degree, a certain

https://doi.org/10.1021/acsomega.3c03201
ACS Omega 2023, 8, 29485−29499

Table 5. Bottom Ash Results from the Reactor Tests (Mean Values for Each Fuel)[a]

			WP100	WSP100	WSP72	WSP60	WSP35	MSP100	MSP52	MSP10
Sintering degree (%)			20.0	84.2	74.9	63.1	51.9	75.5	69.6	62.1
Mean values of the elemental composition expressed as a percentage of the total mass of measured elements (Na, Mg, Al, Si, P, S Cl, K, and Ca) (SEM-EDS) (% m/m: mass percentage)	S1	Al	4.69	0.9	1.32	1.53	3.49	4.08	4.31	5.2
		Si	21.76	49.23	32.99	27.14	30.02	37.99	35.99	37.37
		P	2.76	1.95	3.36	2.82	2.38	2.45	2.97	2.06
		S	0.74	0.82	2.15	2.11	1.88	0.79	0.83	0.56
		Cl	0.1	0.56	0.4	0.37	0.29	0.86	0.46	0.15
		K + Na	14.69	30.06	35.76	36.82	29.65	11.76	13.91	13.68
		Ca + Mg	55.26	16.47	24.01	29.21	32.3	42.07	41.51	40.98
	S2/3	Al	4.25	1.04	1.44	1.78	3.96	4.04	4.27	5.6
		Si	29.94	52.28	37.64	33.48	39.63	46.51	45.28	44.75
		P	2.47	1.99	3.13	2.71	2.02	1.97	2.53	1.65
		S	0.09	0.16	0.29	0.22	0.1	0.12	0.02	0.01
		Cl	0.02	0.03	0	0.01	0.02	0	0.02	0.01
		K + Na	10.29	28.08	34.45	33.9	26.33	9.52	12.53	11.61
		Ca + Mg	52.94	16.42	23.06	27.92	27.95	37.84	35.35	36.38

[a]Due to their chemical similarity and the almost identical role they play in reactions taking place in the ash transformation, the concentrations of K and Na[39] as well as Ca and Mg[40] have been aggregated for all the analysis and included in all the elemental composition tables.

relationship was found between the two parameters, although the variation was very small, given that the combustion temperature for the same fuel was very similar in all tests (see Table 4).

Regarding ash composition, the analysis of the results confirmed that neither the composition of fraction S1 or fraction S2/3 was related to λ, even in the WP100 in which the sintering degree did vary with this parameter.[33]

Because a clear influence of λ on the sintering degree has not been found, except for the WP100, and the composition of each fraction was not affected by this parameter either, for the present analysis, it is interesting to work with mean values and an average composition (see Table 5). The sintering degree is much lower for WP100 than for the rest, and it increases as the percentage of herbaceous increases. The WSP family presents a slightly lower sintering degree than the MSP family, but only in the blended pellets because for pure herbaceous fuels WSP100 has a greater tendency to sinter.

3.3. Deposition. As already mentioned, when analyzing deposition phenomena, only reactor tests with $\lambda > 1$ have been considered, in order to reproduce the operating conditions of actual facilities. Therefore, the number of tests per fuel used in this analysis was much lower, and it was necessary to study all of them together (33 tests between the 8 fuels) in order to know the influence of the operating conditions.

From the analysis of these values, an inverse correlation between DR and λ was obtained.[32] On the other hand, applying the methodology previously indicated, $DR_{Cond.}$ and $DR_{Imp.}$ were estimated in order to determine the contribution of each of the mechanisms to the total DR. Thus, it was found that the increase in λ had opposite effects on each of the two deposition mechanisms: $DR_{Cond.}$ decreases while $DR_{Imp.}$ increases. Both results are, in turn, related to the opposite effect of the λ increase on the combustion temperature and entrainment of solid particles (see refs 32 and 33).

In order to make the analysis of the comparison between fuels independent from the operating parameters, the average values of DR, $DR_{Cond.}$, and $DR_{Imp.}$ of the tests carried out with each fuel are going to be used (see Table 6). It can be seen that for the WP100 the main deposition mechanism is the inertial impact, while for the agropellets, condensation clearly dominates. However, when the percentage of herbaceous in the blend is small (WSP35 and MSP10), the deposition by impact becomes more important.

Regarding the ash composition, the analysis of the results confirmed that it was not linked to the λ value.[33] For this reason, in this work, the average composition of each fraction is used again (Table 6).

4. EXPERIMENTAL TEST IN A COMMERCIAL GRATE FIRED BOILER

4.1. Experimental Design and Test Features. Two tests per each fuel were carried out; first, in order to establish the optimal operation conditions and second, a long run experimental combustion test at steady-state conditions, in which data were obtained to compare with the results of the fixed bed reactor.

These steady-state conditions aim to reach a constant power output of the installation (the goal was to maintain 300 kWth but in the case of MSP family was not possible), with stable combustion parameters during at least 6 h. Table 7 shows the results achieved.

The optimum operating conditions were achieved for an excess of air between 1.5 and 1.65, and the distribution of this air was slightly higher with the primary air (50−57%) than the secondary air (43−50%) for the majority of the tests. This range of configuration was established seeking to assess the best performance for these fuels with a high tendency of sintering.

The efficiency obtained for each fuel was obtained and compared with the reference fuel. For the case of the WSP family, the efficiency is similar to the reference fuel (97−102%), whereas for the MSP family is 15% lower (84−86%) also for all of them, as despite increasing the fuel flow, the power output was below a target value of 300 kW as was mentioned before.

More information about the test features can be found in the Supporting Information, but as mentioned, the main goal satisfied steady-state conditions and this was achieved. Therefore, further analysis of the sintering and deposition phenomena can be compared with the results obtained in the fixed bed reactor for the same fuels.

4.2. Bottom Ash. As indicated in Section 2.4, once each of the tests carried out in the boiler had been completed, the ash deposited on the grate was collected to be weighed and classified in two fractions (S1 and S2/3). After, the elemental composition

https://doi.org/10.1021/acsomega.3c03201
ACS Omega 2023, 8, 29485−29499

Table 6. Deposition Results from the Reactor Tests (Mean of Tests with $\lambda > 1$)

		WP100	WSP100	WSP72	WSP60	WSP35	MSP100	MSP52	MSP10
DR ($g \cdot m^{-2} \cdot h^{-1}$)		4.71	16.49	9.53	7.18	8.53	16.90	15.97	5.87
$DR_{Cond.}$ ($g \cdot m^{-2} \cdot h^{-1}$) (%)[a]		1.9 (40.3)	15.26 (92.5)	8.36 (87.7)	6.53 (90.9)	6.75 (79.1)	16.18 (95.7)	14.7 (92.0)	3.91 (66.6)
$DR_{Imp.}$ ($g \cdot m^{-2} \cdot h^{-1}$) (%)[a]		2.81 (59.8)	1.23 (7.5)	1.17 (12.3)	0.65 (9.1)	1.78 (20.9)	0.72 (4.3)	1.27 (7.9)	1.96 (33.4)
λ		1.49	1.35	1.22	1.36	1.31	1.26	1.11	1.25
T_{if} (°C)		1022	1200	1135	1053	1166	1234	1235	1217
Mean values of the elemental composition expressed as a percentage of the total mass of measured elements (Na, Mg, Al, Si, P, S Cl, K, and Ca) (SEM-EDS) (% m/m: mass percentage)	Al	1.75	0.25	0.22	0.2	0.56	0.16	0.22	0.98
	Si	4.21	1.55	2.53	1.39	3.06	0.67	1.42	3.32
	P	1.97	0.31	0.54	0.31	0.61	0.26	0.33	1.09
	S	6.34	3.21	6.12	6.56	6.68	1.64	1.49	2.28
	Cl	14.75	41.92	35.64	35.94	32.22	47.19	45.19	36.81
	K + Na	34.16	52.07	53.40	53.45	50.61	49.15	49.5	41.36
	Ca + Mg	36.81	0.69	1.56	2.16	6.26	0.94	1.86	14.17

[a]Percentage with respect to DR.

of each fraction was obtained from SEM−EDS. Table 8 includes the percentage of fraction S2/3 with respect to the total ash, i.e., the sintering degree, and the elemental composition of fraction S1 and S2/3.

Table 9 shows the results obtained from the P-XRD analysis of the samples of the fraction S2/3. The percentage of amorphous present in some of the samples has made it impossible to detect some species and quantify those detected (marked in the table with an X).

As can be seen in Table 8, the WP100 has the lowest sintering degree while for agropellets, unlike what happened in the tests carried out in the reactor, it is significantly lower in the MSP family, although the sintering degree also increases with the percentage of herbaceous introduced in the blend in the two families.

As expected, the main elements that appear in both fractions are Si, Ca + Mg, and K + Na. Si content is higher in the S2/3 fraction, while K + Na is in the S1 fraction. The composition of both fractions is directly related to the initial composition of the fuel. Thus, the percentage of Ca + Mg is much higher in WP100 and in the MSP family due to the high percentage of these elements in the fuel ashes (see Table 3), while the K + Na content is significantly higher in both fractions in the WPS family. Regarding the results of the P-XRD (Table 9), it is worth noting the high percentage of amorphous, except in the reference fuel and in the MSP10. It can be stated that this percentage increases with the herbaceous content in the pellet, which is in line with the increase in the sintering degree. In all cases, the presence of high percentages of silicates has been detected in the S2/3 fraction and the presence of quartz has been verified in agropellets, which could be due to a previous contamination of the pellet (presence of sand[11]).

4.3. Deposition Results. In boiler tests, the deposition probe was placed 3 times, with a different sampling ring, during the same test. Figure 3 shows the deposition rates measured from the sample collected in the respective sampling rings and the mean value. It can be verified that the values, for the same fuel, do not vary significantly. These results, in addition to supporting the fact that the conditions remained stable throughout the test, could mean that the DR was similar, not increasing over time. Only the rings of the test carried out with MSP10 present a significant variation. Taking into account these values, in subsequent analyses, the mean value will be used (see Table 11).

Figure 4 shows the mean elemental composition and the range (maximum and minimum values) obtained from SEM−EDS of fly ash deposits collected in the three sampling rings placed during the same test for each fuel. Only a slight variation was detected in this elemental composition (except in the MSP10, where the change was a little bigger). On the other hand, Table 10 shows the crystalline phases and amorphous concentrations detected in the deposits recollected in the three rings of a test, which confirm similar elemental compositions detected previously. Therefore, it was decided to work with the average value (see Table 11) for the following analysis.

As was done in the case of the reactor tests, from the average DR, and applying the methodology indicated in Section 2.4, $DR_{Cond.}$ and $DR_{Imp.}$ were estimated in order to know the contribution of each of the mechanisms to the total DR.

Table 11 shows all the deposition results obtained from the boiler test. In this table, it can be verified that the DR values are much higher than those obtained from the reactor tests (Table 6) mainly due to the different probe locations in both facilities.

https://doi.org/10.1021/acsomega.3c03201
ACS Omega 2023, 8, 29485−29499

Table 7. Operational Parameters and Combustion Commercial Boiler Test Results

Parameter	Units	WP100	WSP100	WSP 72	WSP60	WSP35	MSP100	MSP52	MSP10
Test duration at steady state	h	8.38	6.05	6.23	7.05	7.52	7.75	6.75	6.02
		Boiler Working Conditions							
Flow of biomass	kg/h	76.6	83.1	78.0	79.2	82.6	97.2	83.4	86.0
Average output	kW	304	303	293	303	300	270	265	281
T-gas	°C	791	762	810	852	835	803	759	749
Total air	m^3/h	551	581	538	504	516	507	508	546
Average excess of air	%	66	80	68	53	54	60	50	46[a]
Distribution of the air	horizontal grate primary air (%)	50	55	50	57	56	50	55	55
	secondary air (%)	50	45	50	43	44	50	45	45
		Efficiency							
Compared to WP100[b]	%	100	102	101	97	100	86	84	84[a]

[a]Average excess of air for MSP10 was lower than expected in order to guarantee a good performance as a consequence of problems faced with the air distribution of the installation. [b]The efficiency mentioned in the table is not the efficiency of the combustion, it is the efficiency referred to the reference fuel, WP100.

Table 8. Bottom Ash Results from the Commercial Boiler Tests

			WP100	WSP100	WSP72	WSP60	WSP35	MSP100	MSP52	MSP10
Sintering degree (%)			13.0	68.2	61.1	56.0	47.9	52.2	38.3	31.1
Mean values of the elemental composition expressed as a percentage of the total mass of measured elements (Na, Mg, Al, Si, P, S Cl, K, and Ca) (SEM-EDS) (% m/m: mass percentage)	S1	Al	4.07	0.98	1.15	1.61	3.27	3.97	3.84	5.23
		Si	13.47	43.29	31.93	25.87	35.37	38.83	35.65	33.58
		P	3.01	2.46	3.13	2.82	2.06	2.56	3.17	2.16
		S	1.12	2.08	3.38	3.65	1.90	1.36	1.50	0.98
		Cl	1.37	1.14	0.92	1.07	0.51	1.16	1.35	0.99
		K + Na	21.34	32.69	38.72	40.20	30.65	14.04	16.94	16.46
		Ca + Mg	55.62	17.36	20.77	24.80	26.24	38.09	37.54	40.60
	S2/3	Al	5.33	0.99	1.63	1.84	4.07	4.32	3.96	5.19
		Si	25.94	45.6	38.38	33.40	40.44	48.16	42.87	43.2
		P	2.53	2.37	3.23	2.62	1.91	1.71	2.68	1.90
		S	0.02	1.08	0.89	1.04	0.36	0.17	0.24	0.21
		Cl	0	0.50	0.01	−0.05	0.05	0.05	0	−0.01
		K + Na	13.89	33.09	33.65	34.61	26.90	11.56	15.87	14.36
		Ca + Mg	52.29	16.37	22.20	26.55	26.27	34.03	34.37	35.14

Table 9. Fraction S2/3 Composition

		XRD analysis results								
		Crystalline matter (%)[a]								
Fuel	λ	SiO_2 (quartz)	SiO_2 (cristobalite)	$Ca_2Mg(Si_2O_7)$	$Ca_2(SiO_4)$	$Ca_3(Si_3O_9)$	$KAlSi_2O_6$	$Ca_3Mg(SiO_4)_2$	$K_2Mg_2(SO_4)_3$	Amorphous (%)[b]
WP100	1.65			17.9	24.4			39.2	18.5	0
WSP100	1.80	X[c]				X[c]			X[c]	96.92
WSP72	1.70	X[c]				X[c]			X[c]	93.85
WSP60	1.55					X[c]	X[c]		X[c]	90.49
WSP35	1.55	19.4				47.4	20.3		12.9	53.67
MSP100	1.60	25.8	8.1	9.8		34.5	21.8			74.78
MSP52	1.50	6.2	2.6	7.8		55.5	27.8			49.9
MSP10	1.65	12.3		23.6		36.8	27.3			2.01

[a]Expressed as mass percentages with respect to the total crystalline matter in fraction S2/3. [b]Expressed as mass percentage with respect to the total amount of fraction S2/3. [c]Substances that, being detected, could not be quantified.

Despite this difference, which will be analyzed later, the 100% herbaceous agropellets (WSP100 and MSP100) continue to be those that have a higher DR, especially the latter, while the WP100 presented the lowest DR, as expected. In addition, WP100 and MSP families present a bigger $DR_{Imp.}$ than $DR_{Cond.}$ This difference is more important in the reference fuel, where almost 84% of deposits were due to entrainment of solid particles. For MSP10, this value exceeds 64%. For these fuels, the sintering degree was lower (see Table 8). As already verified in the tests carried out in the reactor[33] and in other similar experiences,[36] there is an inverse relationship between both values, due to sintering preventing entrainment, which, in turn, decreases inertial impact deposition. On the other hand, in the boiler test carried out with fuels of WSP family, the contribution of $DR_{Cond.}$ was bigger (between 74 and 61%), which could be related to a slightly higher combustion temperature.

The elements with a higher concentration in the deposits of the agropellets are K + Na and the second Cl, except for MSP10.

https://doi.org/10.1021/acsomega.3c03201
ACS Omega 2023, 8, 29485−29499

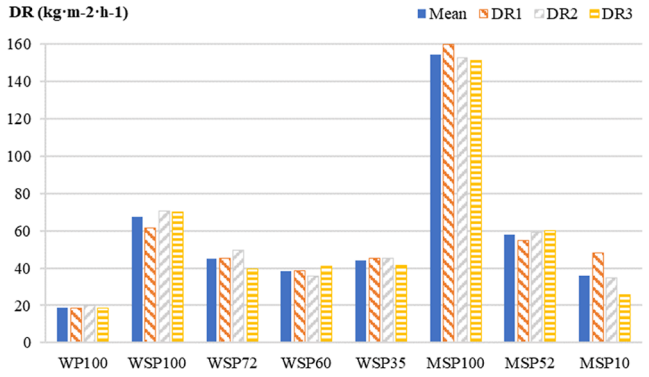

Figure 3. DR in the commercial boiler test ($kg \cdot m^{-2} \cdot h^{-1}$).

In all of them, a high percentage of KCl appears (Table 10) and in the case of the WSP family, K also appears as K_2SO_4. These results are related to deposition by condensation (which includes the deposition by thermophoresis and diffusion after forming aerosols), which confirms the results estimated for the DR_{Cond}. The MSP family, in addition to the previous elements, presents a high content of Si and Ca + Mg, due to the greatest deposition by impact. The SiO_2 and $CaCO_3$ detected by P-XRD (Table 10), which arrives by the entrainment of solid particles, would confirm the high $DR_{Imp.}$ estimated (see Table 11).

In the case of the reference fuel, the high percentage of Ca + Mg is also related to the alkaline-earth content of the fuel ashes (see Table 3). On the other hand, it should be noted that the composition of the deposits for MSP10 is more similar to WP100 than the rest of the agropellets.

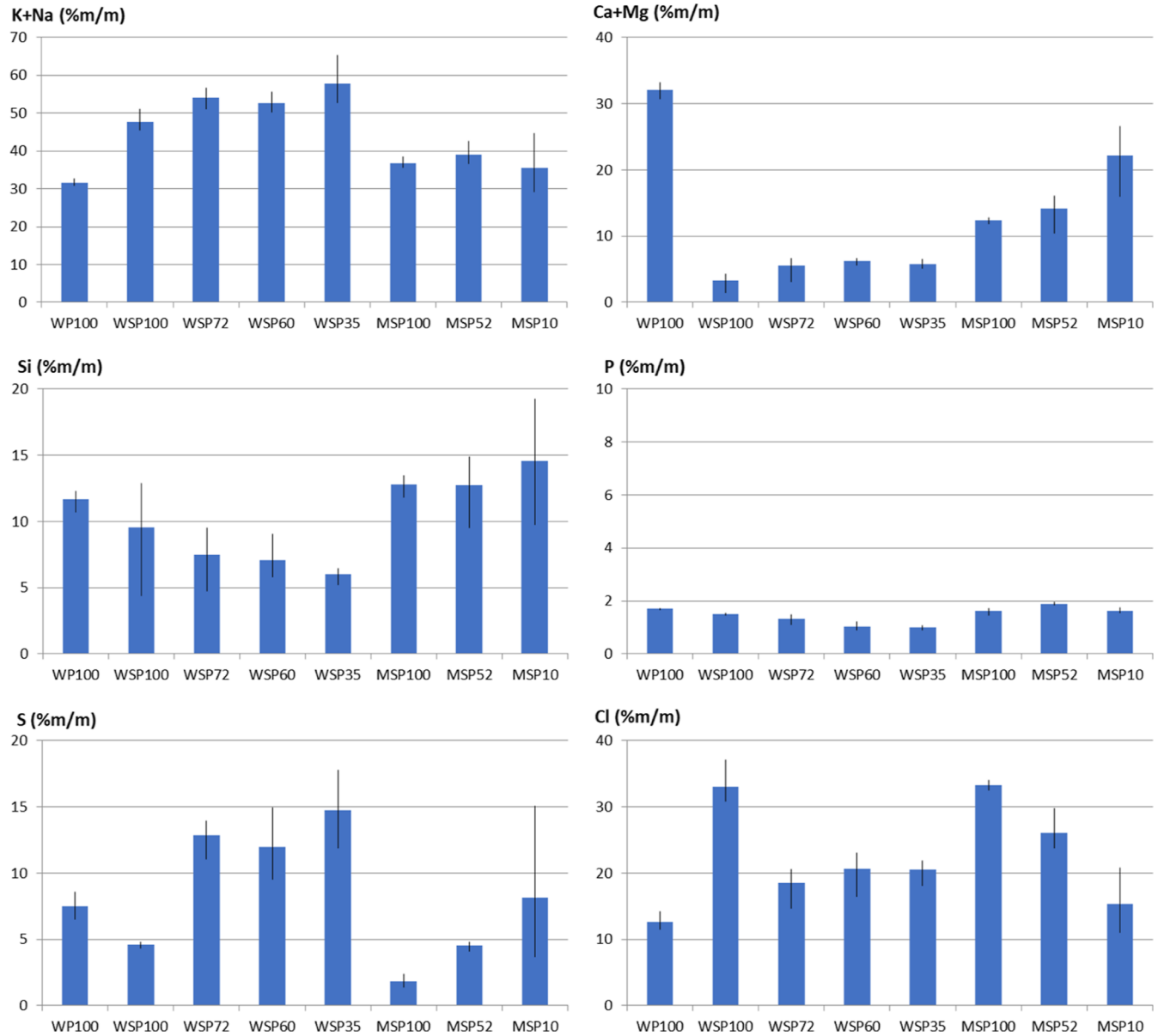

Figure 4. Mass percentage of main elements in deposits, expressed as a percentage of the total mass measured elements (Na, Mg, Al, Si, P, S, Cl, K, and Ca). Mean, maximum, and minimum values for each fuel.

https://doi.org/10.1021/acsomega.3c03201
ACS Omega 2023, 8, 29485−29499

Table 10. Deposit Composition

		XRD analysis results										
		Crystalline matter (%)[a]										
Fuel	λ	KCl	K_2SO_4	SiO_2 (quartz)	$CaCO_3$	$K(Al_3(OH)_6(SO_4)_2)$	$Ca_2Mg(Si_2O_7)$	$Ca_2(SiO_4)$	$Ca_2(Al(AlSi)O_7)$	CaO	MgO	Amorphous (%)[b]
WP100	1.65	7.4		20.1	11.7			18.1	18.3	4.4	19.8	40.78
		8.1		23.6	12			18.3	12.1	5	21	46.19
		10.7		23.5	11.8			18.3	13.3	3.9	18.6	31.8
WSP100	1.80	79	21									8.96
		79.1	20.9									23.23
		76.3	23.7									22.96
WSP72	1.70	51.7	48.3									43.6
		41.8	58.2									15.76
		35	65									25.79
WPS60	1.55	52.8	47.2									33.75
		43.5	56.5									22.45
		55	45									36.72
WPS35	1.55	30.8	40.5	28.7								23.59
		26.7	56.1	17.2								23.05
		32.7	44	23.3								26.8
MSP100	1.60	47.8		41.3	10.9							24.65
		35.8		52	12.1							18.3
		32.3		53.1	14.5							23.39
MSP52	1.50	17.4		36.3	13.4	14.1	10	8.8				38.11
		26.5		30.3	13.5	8.7	13.3	7.6				45.28
		22.5		43	20		14.4					45.41
MSP10	1.65	5.6		75.2	13.3					5.9		27.97
		10.7		62.2	19.8					7.3		52.1
		12.6		32.4	23.6				24.7	6.8		60.97

[a]Expressed as mass percentages with respect to the total crystalline matter in fraction S2/3. [b]Expressed as mass percentage with respect to the total amount of fraction S2/3.

5. RESULT COMPARISON AND VALIDATION OF THE EXPERIMENTAL INSTALLATION

In this section, the results obtained in both installations are compared in order to verify if the reactor (results in Sections 3.2 and 3.3) adequately reproduces the ash behavior in a commercial boiler (results in Sections 4.2 and 4.3).

Regarding the sintering degree, Figure 5 shows the mean fraction S2/3 in the reactor tests (Table 5) versus the one obtained in boiler tests (Table 8). There is a statistically significant correlation ($r = 0.84$ and $p = 0.0081$) between both values.

It can be verified that these values are somewhat higher in the reactor, which may be related with differences in the combustion temperature. It must be taken into account that in the tests carried out in the boiler, the operation conditions were adjusted to control sintering problems, which could not be done in the case of the tests in the reactor. Thus, for the MSP family, the combustion temperatures in the reactor tests were very high (mean $T_{if} > 1200$ °C, see Table 4), which increased sintering problems. For these fuels, the difference between the results in the reactor and the boiler is greater than for the rest of the fuels. In any case, the relationship continued to hold in such a way that the most problematic fuel in the reactor was also in the boiler and vice versa.

Regarding the bottom ash composition, the elemental composition of the two fractions that were obtained from bottom ash (S1 and S2/3) in the tests carried out in the boiler with each fuel (Table 8) have been compared with the mean value obtained in the reactor tests (Table 5). Figures 6 and 7 present this comparison for the main elements that compose fractions S1 and S2/3, respectively.

As reflected in these figures, the composition is very similar, with no significant changes in any of the elements. It has been proven that there is a statistically significant relationship between the percentages of each element in the ash fractions of both facilities (see Table 12).

Because both the composition and quantity of fraction S2/3 (sintering degree) are similar in the tests carried out in the reactor and in the boiler, the conclusions obtained from the reactor tests about the sintering behavior of fuels can be transferred to commercial equipment.

Regarding the DR, Figure 8 shows the mean value obtained in the reactor tests (Table 6) versus the mean value obtained in boiler tests (Table 11). There is a correlation ($r = 0.75$; $p = 0.0309$) between both values, but, in this case, DR in the boiler is much higher than in the reactor (between 4 and 6 times higher in the boiler and up to 9 times for the MSP10).

These disparities are mainly due to the different locations of the deposition probe in both facilities. First, in the boiler the entire surface of the probe ring is exposed to gas flow, which causes DR to have higher values. In addition, the probe is located in the combustion chamber, much more directly exposed to the gas flow, which have just left the bed entraining large amounts of ash. This fact has implied that the $DR_{Imp.}$ in the boiler have been much higher than the one in the reactor (see Figure 9). In this case, no statistically significant relationship was found between the two values ($r = 0.42$; $p = 0.3049$).

Another factor must be taken into account when the differences detected in DR_{imp} are analyzed: the influence of

https://doi.org/10.1021/acsomega.3c03201
ACS Omega 2023, 8, 29485−29499

Table 11. Deposition Results in Commercial Boiler Tests

		WP100	WSP100	WSP72	WSP60	WSP35	MSP100	MSP52	MSP10
DR ($g \cdot m^{-2} \cdot h^{-1}$)		18.91	67.34	44.81	38.31	44.07	154.53	57.98	36.15
$DR_{Cond.}$ ($g \cdot m^{-2} \cdot h^{-1}$) (%)[a]		3.09 (16.3)	46.01 (68.3)	31.03 (69.2)	23.51 (61.4)	32.49 (73.7)	76.13 (49.3)	27.82 (48.0)	12.87 (35.6)
$DR_{Imp.}$ ($g \cdot m^{-2} \cdot h^{-1}$) (%)[a]		15.82 (83.7)	21.33 (31.7)	13.78 (30.8)	14.81 (38.7)	11.57 (26.3)	78.40 (50.7)	30.16 (52.0)	23.28 (64.4)
Mean values of the elemental composition expressed as a percentage of the total mass of measured elements (Na, Mg, Al, Si, P, S Cl, K, and Ca) (SEM-EDS) (% m/m: mass percentage)	Al	2.79	0.37	0.33	0.44	0.72	1.43	1.54	2.72
	Si	11.67	9.53	7.48	7.10	5.99	12.8	12.74	14.53
	P	1.7	1.51	1.33	1.04	1.01	1.63	1.9	1.63
	S	7.51	4.58	12.84	11.95	14.75	1.82	4.53	8.14
	Cl	12.62	32.97	18.48	20.67	20.47	33.25	26.11	15.28)
	K + Na	31.6	47.73	54.06	52.6	57.79	36.64	39.05	35.51
	Ca + Mg	32.11	3.31	5.48	6.21	5.76	12.43	14.13	22.19

[a]Percentage with respect to DR.

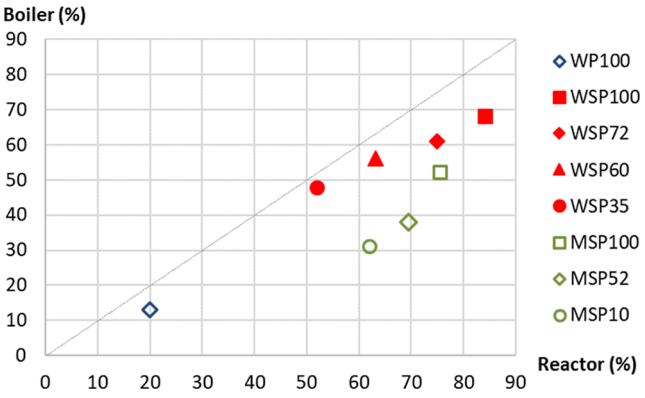

Figure 5. Sintering degree of bottom ash in boiler tests versus average sintering degree of bottom ash in reactor tests for each fuel.

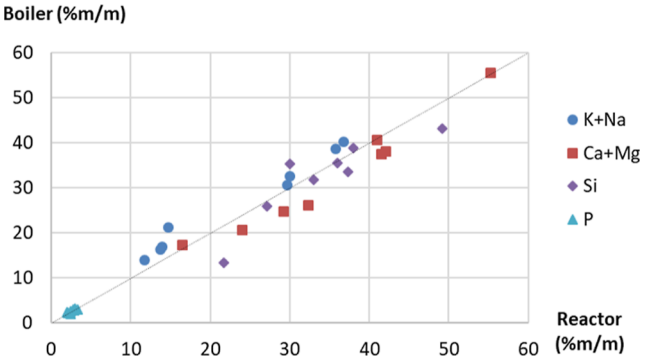

Figure 6. Elemental composition (SEM−EDS) of fraction S1 collected in reactor tests (mean value of all tests) versus fraction S1 collected in boiler tests for each fuel, expressed as a percentage of the total mass of measured elements (Na, Mg, Al, Si, P, S, Cl, K, and Ca).

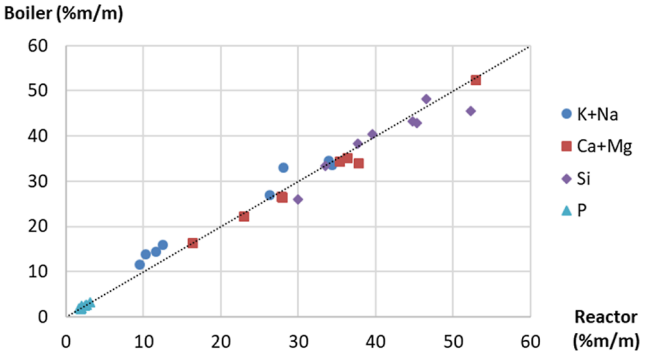

Figure 7. Elemental composition (SEM−EDS) of fraction S2/3 collected in reactor tests (mean value of all tests) versus fraction S2/3 collected in boiler tests for each fuel, expressed as a percentage of the total mass of measured elements (Na, Mg, Al, Si, P, S, Cl, K, and Ca).

bottom ash sintering degree. As already pointed out above, there is an inverse relationship between both values. In order to filter the effect that the location of the probe has on the results, it is more appropriate to use the percentage of deposits due to the inertial impact of entrained particles with respect to the total collected in the ring (DRi_{mp} in percent). Figure 10 represents this value against the sintering degree. It can be verified that the same relationship exists between these two values in the tests carried out on both devices, with a statistically significant correlation ($r = 0.90$; $p < 0.00001$). Therefore, the higher DR_{imp} detected in the boiler tests is related not only to the location of

https://doi.org/10.1021/acsomega.3c03201
ACS Omega 2023, 8, 29485−29499

Table 12. Pearson's Coefficient (r) and p-Values (p) of the Correlations between the Concentrations of Each Element in the Bottom Ash Fractions Collected in Boiler Tests and in Reactor Tests

	K + Na		Ca + Mg		Si		P	
	r	p	r	p	r	p	r	p
S1	0.99	<0.0001	0.98	<0.0001	0.89	0.0033	0.83	0.0103
S2/3	0.99	<0.0001	1	<0.0001	0.92	0.0010	0.91	0.0015

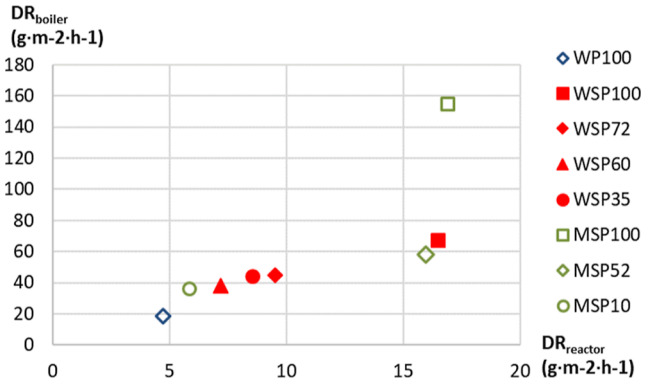

Figure 8. Mean DR in boiler tests versus mean DR in reactor tests for each fuel.

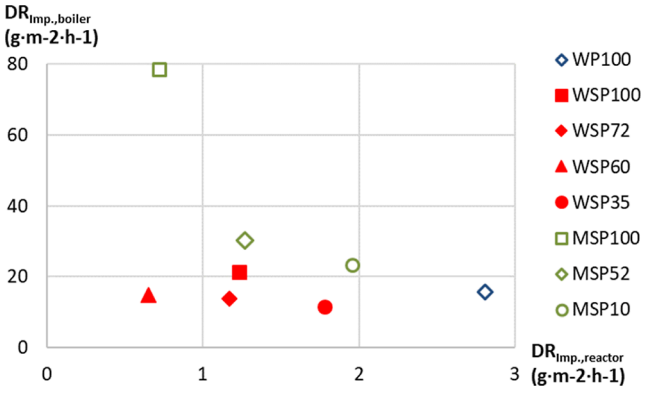

Figure 9. Mean DR by inertial impact in boiler tests versus mean DR by inertial impact in reactor tests for each fuel.

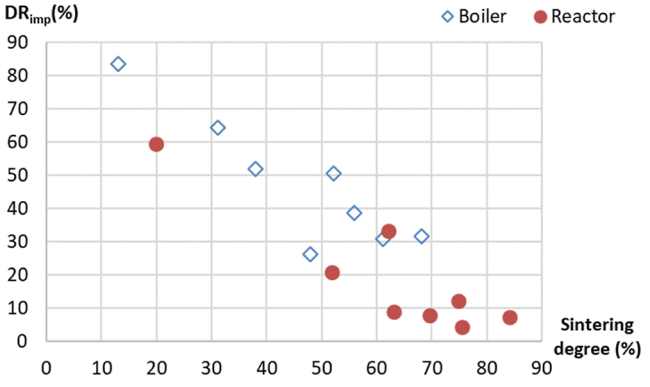

Figure 10. Mean DR by inertial impact in % in all the tests versus sintering degree of bottom ash in boiler tests and average sintering degree of bottom ash in reactor tests.

the probe, which has led to a greater amount of total deposits, but also to the fact that the bottom ash sintering degree was lower in the boiler tests.

When the $DR_{Cond.}$ is analyzed, differences are also found between the values obtained in both facilities (see Figure 11) again mainly due to the different situations of the probe ring. However, in this case, a statistically significant correlation has been found ($r = 0.83$; $p = 0.0112$).

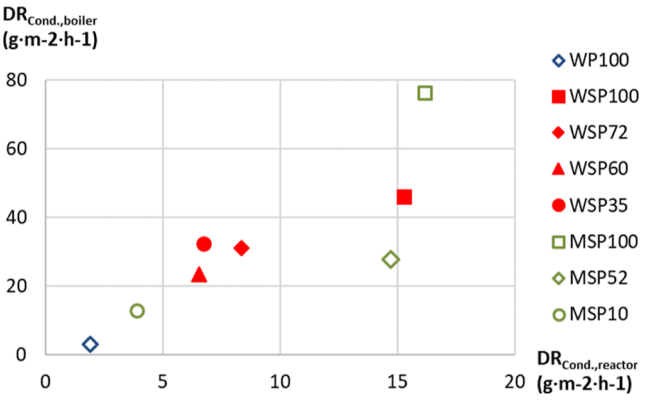

Figure 11. Mean DR by condensation in boiler tests versus mean DR by condensation in reactor tests for each fuel.

Regarding deposit composition, the mean elemental composition of the deposits obtained for each fuel in the tests carried out in the boiler (Table 11) has been compared with the mean value obtained in the reactor tests (Table 6). Figure 12 presents this comparison for the main elements that compose these deposits.

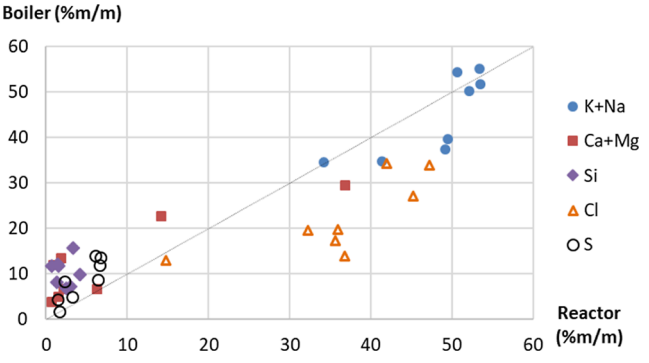

Figure 12. Elemental composition (SEM−EDS) of deposits collected in reactor tests (mean value of all tests) versus deposits collected in boiler tests (mean of three sampling rings) for each fuel, expressed as a percentage of the total mass of measured elements (Na, Mg, Al, Si, P, S, Cl, K, and Ca).

Statistically significant correlations were found for each of the elements except for Si (see Table 13). This element has a higher concentration in the boiler deposits due to the higher deposition by impact associated with the location of the probe that has been commented on previously.

https://doi.org/10.1021/acsomega.3c03201
ACS Omega 2023, 8, 29485−29499

Table 13. Pearson's Coefficient (r) and p-Values (p) of the Correlations between the Concentrations of Each Element in Deposits Collected in Boiler Tests and in Reactor Tests

	K + Na		Ca + Mg		Si		Cl		S	
	r	p	r	p	r	p	r	p	r	p
Deposits	0.78	0.0218	0.88	0.0040	0.07	0.8718	0.76	0.0302	0.86	0.0061

On the other hand, the lower concentration of Cl and the higher of S stands out in the boiler tests, which suggests a greater deposition by condensation in the form of sulfates and a lower one in the form of chlorides. The P-XRD results already seem to confirm these findings (you can compare the results of the deposits in the boiler case, as shown in Table 10, with those of the reactor case, as shown in ref 36). This difference in behavior may be related to the fact that a greater excess of air was used in the boiler, which implies lower combustion temperatures and, therefore, a lower release of Cl and a higher release of S.[41]

In any case, it must be taken into account that the deposition of each compound is also affected by the temperature of the gases, their gradients, and their fluid dynamics, which are conditioned by the position of the probe in the boiler and in the reactor. Despite all this, the trends of the results obtained between both facilities are similar.

6. CONCLUSIONS

Eight different pellets produced in an IBLC were tested in a commercial boiler. The results were compared with the ones obtained in a previous test campaign carried out with the same fuels in a fixed bed reactor at the lab scale seeking to validate the results and conclusions obtained in the latter. Agropellets achieved a good performance in all cases during the tests carried out in the boiler considering the efficiency reached and the emissions reported even though agropellets produced with wheat straw (WSP family) performed slightly better.

Furthermore, and as a main objective of this paper, their ash behavior was also assessed (sintering and deposition) by comparing the results in both installations in order to validate the usefulness of the experimental tests carried out in the fixed bed reactor.

The following conclusions can be drawn from the analysis and comparison of the results obtained:

- A very similar elemental composition was found in fractions S1 and S2/3 of bottom ash and in deposits collected in both facilities, even though operational conditions, such as the combustion temperature, were not the same, which may indicate that the reactor allows reproducing a representative combustion performance. In fact, the only meaningful variations detected in the deposits' compositions (lower chlorine and higher sulfur composition in boiler test samples) seem to be directly related to the deposition probe location and the excess of air.
- The similarities observed regarding the ash composition in both the boiler and reactor enable one to use the samples collected from the reactor to derive information regarding the composition that could be obtained from the ash collected from the boiler. Therefore, reactors' tests enable one to predict possible problems that could arise associated with corrosion occurrence for instance or to assess the ash potential for different applications (i.e., fertilizer) without requiring the performance of long and complex tests in the boiler while allowing to increase the number of tests performed and the typologies of fuels that can be tested.
- Concerning sintering, the results presented the same trends both in the reactor and the boiler tests. In addition, it has been corroborated that carrying out the tests in this type of reactor gives a representative insight of the worst sintering degree that can be expected when working with these fuels in commercial boilers. These facilities allow one to optimize the operating conditions according to the fuel in a better way than an experimental reactor. In this sense, the sintering degree can be reduced as confirmed in this work although keeping in mind that this decrease will depend on the type of boiler and the optimization conditions achieved in for each fuel.
- Regarding the fuel deposition trend, although the values obtained were very different due to the probes being placed in different locations in each facility, the results obtained indicate a statistically significant direct relationship between the DR values.
- After analyzing separately deposition mechanisms, the percentage of deposits generated by the inertial impact as against the total was found to be inversely related with the sintering degree, keeping the same relationship in both facilities. Taking into account that a biofuel's bottom ash sintering degree is foreseen to be lower in the commercial boiler, deposition by inertial impact is expected to be higher in the commercial boiler (caused by a higher bottom ash entrainment) as it was previously pointed out, thus excess of air will need to be adjusted according to this fact.

Finally, the main conclusion of this study is that both sintering and deposition phenomena seem to be predictable based on the results obtained in reactor experiments. This fact can simplify the testing process, save significant time and effort, and allow for the behavior of more biofuels to be predicted. In addition, it would mean that only those biofuels that exhibit favorable behavior in reactor experiments, which would be tested in commercial boilers.

■ ASSOCIATED CONTENT

Supporting Information

The Supporting Information is available free of charge at https://pubs.acs.org/doi/10.1021/acsomega.3c03201.

Comprehensive insights into the experimental design and test features conducted in the commercial grate boiler, combustion performance of eight distinct agropellet varieties under real-world operational conditions, boiler configuration and operating parameters, and data on combustion efficiency and emission profiles achieved throughout the combustion process (PDF)

https://doi.org/10.1021/acsomega.3c03201
ACS Omega 2023, 8, 29485−29499

AUTHOR INFORMATION

Corresponding Author

Sebastián Zapata − *CIRCE—Technology Centre, E-50018 Zaragoza, Spain;* orcid.org/0000-0002-5058-1005; Email: szapata@fcirce.es

Authors

Paula Canalís − *University of Zaragoza, E-50018 Zaragoza, Spain;* orcid.org/0000-0002-5037-7047

Javier Royo − *University of Zaragoza, E-50018 Zaragoza, Spain;* orcid.org/0000-0003-4631-6994

Maider Gómez − *CIRCE—Technology Centre, E-50018 Zaragoza, Spain*

Carmen Bartolomé − *CIRCE—Technology Centre, E-50018 Zaragoza, Spain;* orcid.org/0000-0002-6210-1099

Complete contact information is available at: https://pubs.acs.org/10.1021/acsomega.3c03201

Notes

The authors declare no competing financial interest.

ACKNOWLEDGMENTS

This publication is part of a project that has received funding from the European Union's Horizon 2020 research and innovation program under grant agreement no. 727961. The work was performed in the framework of the European project AGROinLOG (grant agreement no. 727961) "Demonstration of innovative integrated biomass logistics centers for the Agro-industry sector in Europe". http://www.agroinlogh2020.eu/. This publication was partially funded by the European project BRANCHES (grant agreement no. 101000375) Boosting Rural Bioeconomy Networks following multi-actor approaches and the Government of Aragon in Spain. The authors also would like to acknowledge the use of the Servicio General de Apoyo a la Investigación—SAI, Universidad de Zaragoza.

ABBREVIATIONS

DR	deposition rate ($g{\cdot}m^{-2}{\cdot}h^{-1}$)
$DR_{Cond.}$	deposition rate by condensation ($g{\cdot}m^{-2}{\cdot}h^{-1}$)
$DR_{Imp.}$	deposition rate by inertial impact ($g{\cdot}m^{-2}{\cdot}h^{-1}$)
IBLC	integrated biomass logistic center
LHV	low heating value
MSP	maize stalk pellet (pure or blended with forestry wood)
p	*p*-value (Pearson's correlation)
PA	air mass flow by unit area of the grate
r	Pearson's correlation coefficient
S1	not sintered ash fraction
S2	low sintered ash fraction
S2/3	fraction S2 plus fraction S3
S3	high sintered ash fraction
T_a	inlet air temperature in the reactor
T-Amb	ambient temperature
TC	thermocouple
TC*i*	temperature registered by the thermocouple located in position *i*
T-gas	commercial boiler combustion gas temperature (combustion chamber outlet)
T_{if}	mean flame temperature
WP	wood pellet
WSP	wheat straw pellet (pure or blended with forestry wood)
λ	excess air ratio

REFERENCES

(1) Fit for 55. https://www.consilium.europa.eu/ accessed Dec 15, 2022.

(2) *Directive (EU) 2018/2001 of the European Parliament and of the Council of 11 December 2018 on the Promotion of the Use of Energy from Renewable Sources*, 2018.

(3) Carvalho, L.; Wopienka, E.; Pointner, C.; Lundgren, J.; Verma, V. K.; Haslinger, W.; Schmidl, C. Performance of a pellet boiler fired with agricultural fuels. *Appl. Energy* **2013**, *104*, 286−296.

(4) Wang, L.; Skjevrak, G.; Hustad, J. E.; Gronli, M.; Skreiberg, O. Effects of Additives on Barley Straw and Husk Ashes Sintering Characteristics. *Energy Procedia* **2012**, *20*, 30−39.

(5) Sippula, O.; Hytönen, K.; Tissari, J.; Raunemaa, T.; Jokiniemi, J. Effect of Wood Fuel on the Emissions from a Top-Feed Pellet Stove. *Energy Fuels* **2007**, *21*, 1151−1160.

(6) Houshfar, E.; Lovas, T.; Skreiberg, O. Experimental Investigation on NOX Reduction by Primary Measures in Biomass Combustion: Straw, Peat, Sewage Sludge, Forest Residues and Wood Pellets. *Energies* **2012**, *5*, 270−290.

(7) Díaz-Ramírez, M.; Sebastian, F.; Royo, J.; Rezeau, A. Influencing factors on NOX emission level during grate conversion of three pelletized energy crops. *Appl. Energy* **2014**, *115*, 360−373.

(8) Glarborg, P.; Marshall, P. Mechanism and modeling of the formation of gaseous alkali sulfates. *Combust. Flame* **2005**, *141*, 22−39.

(9) Garba, M. U.; Ingham, D. B.; Ma, L.; Porter, R. T. J.; Pourkashnian, M.; Tan, H. Z.; Williams, A. Prediction of Potassium Chloride Sulfation and Its Effect on Deposition in Biomass-Fired Boilers. *Energy Fuels* **2012**, *26*, 6501−6508.

(10) Pyykönen, J.; Jokiniemi, J. Modelling alkali chloride superheater deposition and its implications. *Fuel Process. Technol.* **2003**, *80*, 225−262.

(11) Niu, Y.; Tan, H.; Hui, S. Ash-related issues during biomass combustion: Alkali-induced slagging, silicate melt-induced slagging (ash fusion), agglomeration, corrosion, ash utilization, and related countermeasures. *Prog. Energy Combust. Sci.* **2016**, *52*, 1−61.

(12) Capablo, J. Formation of alkali salt deposits in biomass combustion. *Fuel Process. Technol.* **2016**, *153*, 58−73.

(13) Eric, A.; Nemoda, S.; Komatina, M.; Dakić, D.; Repić, B. Experimental investigation on the kinetics of biomass combustion in vertical tube reactor. *J. Energy Inst.* **2019**, *92*, 1077−1090.

(14) Regueiro, A.; Patiño, D.; Granada, E.; Porteiro, J. Experimental study on the fouling behaviour of an underfeed fixed-bed biomass combustor. *Applied Thermal Engineering* **2017**, *112*, 523−533.

(15) Porteiro, J.; Patiño, D.; Collazo, J.; Granada, E.; Moran, J.; Miguez, J. L. Experimental analysis of the ignition front propagation of several biomass fuels in a fixed-bed combustor. *Fuel* **2010**, *89*, 26−35.

(16) Ryu, C.; Yang, Y. B.; Khor, A.; Yates, N. E.; Sharifi, V. N.; Swithenbank, J. Effect of fuel properties on biomass combustion: Part I. Experiments − fuel type, equivalence ratio and particle size. *Fuel* **2006**, *85*, 1039−1046.

(17) Li, G.; Li, S.; Xu, X.; Huang, Q.; Yao, Q. Dynamic behavior of biomass ash deposition in a 25 kW one-dimensional down-fired combustor. *Energy Fuels* **2013**, *28*, 219−227.

(18) Theis, M.; Skrifvars, B. J.; Hupa, M.; Tran, H. Fouling tendency of ash resulting from burning mixtures of biofuels. Part 1: deposition rates. *Fuel* **2006**, *85*, 1125−1130.

(19) Fernández-Llorente, M. J.; Escalada-Cuadrado, R.; Murillo-Laplaza, J. M.; Carrasco-García, J. E. Combustion in bubbling fluidised bed with bed material of limestone to reduce the biomass ash agglomeration and sintering. *Fuel* **2006**, *85*, 2081−2092.

(20) Díaz-Ramírez, M.; Frandsen, F. J.; Glarborg, P.; Sebastian, F.; Royo, J. Partitioning of K, Cl, S and P during combustion of poplar and brassica energy crops. *Fuel* **2014**, *134*, 209−219.

(21) Royo, J.; Canalís, P.; Quintana, D.; Díaz-Ramírez, M.; Sin, A.; Rezeau, A. Experimental study on the ash behaviour in combustion of pelletized residual agricultural biomass. *Fuel* **2019**, *239*, 991−1000.

(22) Hupa, M. Ash-related issues in fluidized-bed combustion of biomasses: recent research highlights. *Energy Fuels* **2011**, *26*, 4−14.

(23) Madhiyanon, T.; Sathitruangsak, P.; Sungworagarn, S.; Pipatmanomai, S.; Tia, S. A pilot-scale investigation of ash and deposition formation during oil-palm empty-fruit-bunch (EFB) combustion. *Fuel Process. Technol.* **2012**, *96*, 250−264.
(24) Teixeira, P.; Lopes, H.; Gulyurtlu, I.; Lapa, N.; Abelha, P. Evaluation of slagging and fouling tendency during biomass co-firing with coal in a fluidized bed. *Biomass Bioenergy* **2012**, *39*, 192−203.
(25) Öhman, M.; Boman, C.; Hedman, H.; Nordin, A.; Boström, D. Slagging tendencies of wood pellet ash during combustion in residential pellet burners. *Biomass Bioenergy* **2004**, *27*, 585−596.
(26) Sommersacher, P.; Brunner, T.; Obernberger, I. Fuel indexes: A novel method for the evaluation of relevant combustion properties of new biomass fuels. *Energy Fuels* **2012**, *26*, 380−390.
(27) Lindström, E.; Sandström, M.; Boström, D.; Öhman, M. Slagging Characteristics during Combustion of Cereal Grains Rich in Phosphorus. *Energy Fuels* **2007**, *21*, 710−717.
(28) Díaz-Ramírez, M.; Sebastián, F.; Royo, J.; Rezeau, A. Combustion requirements for conversion of ash-rich novel energy crops in a 250 kWth multifuel grate fired system. *Energy* **2012**, *46*, 636−643.
(29) Zeng, T.; Pollex, A.; Weller, N.; Lenz, V.; Nelles, M. Blended biomass pellets as fuel for small scale combustion appliances: Effect of blending on slag formation in the bottom ash and pre-evaluation options. *Fuel* **2018**, *212*, 108−116.
(30) Zhou, H.; Jensen, P. A.; Frandsen, F. J. Dynamic mechanistic model of superheater deposit growth and shedding in a biomass fired grate boiler. *Fuel* **2007**, *86*, 1519−1533.
(31) Patiño, D.; Crespo, B.; Porteiro, J.; Míguez, J. L. Experimental analysis of fouling rates in two small-scale domestic boilers. *Appl. Therm. Eng.* **2016**, *100*, 849−860.
(32) Zapata, S.; Gómez, M.; Bartolomé, C.; Canalís, P.; Royo, J. Ash Behaviour during Combustion of Agropellets Produced by an Agro-Industry—Part 1: Blends Design and Experimental Tests Results. *Energies* **2022**, *15*, 1479.
(33) Royo, J.; Canalís, P.; Zapata, S.; Gómez, M.; Bartolomé, C. Ash Behaviour during Combustion of Agropellets Produced by an Agro-Industry—Part 2: Chemical Characterization of Sintering and Deposition. *Energies* **2022**, *15*, 1499.
(34) *Website European Project AGROinLOG: Demonstration of Innovative Integrated Biomass Logistics Centres for the Agro-Industry Sector in Europe*, 2022. Thurs. 1 Sept. 2022. https://www.fcirce.es/en/renewable-energy/agroinlog.
(35) *D3.7_Success Case of an IBLC into an Agroindustry of the Animal Feed Sector. May, 2020. Project AGROinLOG "Demonstration of Innovative Integrated Biomass Logistics Centres for the Agro-Industry Sector in Europe" Grant agreement: 727961*, 2020. https://cordis.europa.eu/project/id/727961/results.
(36) Royo, J.; Canalís, P.; Quintana, D. Chemical study of fly ash deposition in combustion of pelletized residual agricultural biomass. *Fuel* **2020**, *268*, 117228.
(37) Díaz-Ramírez, M.; Boman, C.; Sebastian, F.; Royo, J.; Xiong, S.; Boström, D. Ash Characterization and Transformation Behavior of the Fixed-Bed Combustion of Novel Crops: Poplar, Brassica, and Cassava Fuels. *Energy Fuels* **2012**, *26*, 3218−3229.
(38) Royo, J.; Canalís, P.; Quintana, D. Chemical study of bottom ash sintering in combustion of pelletized residual agricultural biomass. *Fuel* **2022**, *310*, 122145.
(39) Boström, D.; Skoglund, N.; Grimm, A.; Boman, C.; Ohman, M.; Brostrom, M.; Backman, R. Ash transformation chemistry during combustion of biomass. *Energy Fuels* **2012**, *26*, 85−93.
(40) Zevenhoven, M.; Yrjas, P.; Skrifvars, B. J.; Hupa, M. Characterization of ash-forming matter in various solid fuels by selective leaching and its implications for fluidized-bed combustion. *Energy Fuels* **2012**, *26*, 6366−6386.
(41) Leppänen, A. Modeling Fume Particle Dynamics and Deposition with Alkali Metal Chemistry in Kraft Recovery Boilers, Ph.D. Thesis, Tampere University of Technology, 2015. Publication 1273.

https://doi.org/10.1021/acsomega.3c03201
ACS Omega 2023, 8, 29485−29499